Antarctic Science 12 (1): 20–32 (2000) © British Antarctic Survey Printed in the United Kingdom

Optimizing models for remotely estimating primary production in Antarctic coastal waters

H.M. DIERSSEN[1], M. VERNET[2] and R.C. SMITH[1]

[1]*Department of Geography, Institute for Computational Earth System Science, University of California at Santa Barbara, Santa Barbara, CA 93106, USA*

[2]*Marine Research Division, Scripps Institution of Oceanography, University of California, San Diego, La Jolla, CA 92093, USA*

Abstract: Primary productivity and associated biogeochemical fluxes within the Southern Ocean are globally significant, sensitive to change and poorly known compared to temperate marine ecosystems. We present seasonal time series data of chlorophyll *a*, primary productivity and in-water irradiance measured in the coastal waters of the Western Antarctica Peninsula and build upon existing models to provide a more optimum parameterization for the estimation of primary productivity in Antarctic coastal waters. These and other data provide strong evidence that bio-optical characteristics and phytoplankton productivity in Antarctic waters are different from temperate waters. For these waters we show that over 60% of the variability in primary production can be explained by the surface chlorophyll *a* concentration alone, a characteristic, which lends itself to remote sensing models. If chlorophyll *a* concentrations are accurately determined, then the largest source of error (13–18%) results from estimates of the photoadaptive variable (P^B_{opt}). Further, the overall magnitude of P^B_{opt} is low (median 1.09 mg C mg chl^{-1} h^{-1}) for these data compared to other regions and generally fits that expected for a cold water system. However, the variability of P^B_{opt} over the course of a season (0.4 to 3 mg C mg chl^{-1} h^{-1}) is not consistently correlated with other possible environmental parameters, such as chlorophyll, sea surface temperature, incident irradiance, day length, salinity, or taxonomic composition. Nonetheless, by tuning a standard depth-integrated primary productivity model to fit representative P^B_{opt} values and the relatively uniform chlorophyll-normalized production profile found in these waters, we can improve the model to account for approximately 72–73% variability in primary production both for our data as well as for independent historic Antarctic data.

Received 1 October 1998, accepted 27 July 1999

Key words: Antarctic Peninsula, bio-optical model, Palmer LTER, primary production, SeaWiFS, Southern Ocean

Introduction

In order to understand and quantify global oceanic primary productivity and the flux of carbon in the world's oceans, considerable effort has been directed towards developing satellite algorithms to model this production. Such algorithms may be used to estimate the rate of primary productivity from the concentration of biomass in a water column using different scales of integration (e.g. depth, time, and wavelength). Aside from the simplest empirical correlation between chlorophyll and primary productivity (Smith *et al.* 1982), all primary productivity models generally invoke some photoadaptive variable that changes linearly with biomass concentration (e.g. the maximum carbon fixation rate within a water column P^B_{opt}, water-column averaged light utilization Ψ, etc.). Recently, Behrenfeld & Falkowski (1997a) have shown that given the same biomass concentrations, much of the error in primary productivity models is associated with uncertainties in the photoadaptive variable and not with the specific structure of the algorithm. These workers suggest that improvements in productivity algorithm performance will depend less on improved mathematical formulations and more on improved understanding of phytoplankton ecology and photoadaptive variability (Longhurst *et al.* 1995, Antoine *et al.* 1996, Behrenfeld & Falkowski 1997b).

Antarctic coastal waters are much colder than temperate waters, and the annual range of temperature variability is relatively small (-2°C to +2°C). However, the Antarctic marine ecosystem is characterized by large variations in solar radiation both on a daily and a seasonal basis. Water column stability and the opposing influence of high winds and consequent deep mixing are also highly variable and have long been recognized as important controlling factors for phytoplankton biomass build-up (Hart 1934, Mitchell & Holm-Hansen 1991, Nelson & Smith 1991, Priddle *et al.* 1994). Indeed, wind forcing, atmospheric variability, sea ice and snow cover, and changing ocean optical properties combine to cause a highly variable light regime for Antarctic phytoplankton. In spite of often unfavourable conditions, high biomass concentrations (> 30 mg chl m^{-3}) have been observed (Hart 1934, El-Sayed 1978, Smith *et al.* 1996a).

How the Antarctic phytoplankton respond to this variable environment, both on a daily and seasonal basis, remains a key question in our attempt to understand primary productivity in this region. Past research has shown that the phytoplankton

are generally adapted to the low light and low temperatures (El-Sayed 1978, Tilzer *et al.* 1986, Smith & Sakshaug 1990, Smith *et al.* 1996a), but the phytoplankton ecology and inherent variability in photoadaptation is far from understood. The efficiency with which phytoplankton use light for primary production is determined both by the extent to which aquatic plants succeed in competing with the other components of the system for quanta and by the efficiency with which the absorbed light energy is converted to chemical energy. Here we make use of a time series of biological and optical data collected in conjunction with the Palmer Long-Term Ecological Research (LTER) project (Smith *et al.* 1995) to:

1) investigate the underlying causes of photoadaptive variability of phytoplankton over the course of the growing season,
2) evaluate the relative accuracy of productivity models, and
3) inquire how best to parameterize a productivity model so as to enhance model performance in Antarctic coastal waters.

Methods

We analyse time series data obtained in 1994–95 and 1995–96 from two in-shore stations (B and E) near Palmer Station, Antarctica (64°46'S, 64°03'W) and from a larger area, the Palmer LTER large scale study grid, during a January–February 1995 cruise (Fig. 1). Nearshore sampling was conducted weekly from approximately November to the end of March (weather and ice permitting) for both field seasons at stations B and E (Waters & Smith 1992). Samples were collected at depths corresponding to the following percent surface irradiance as measured using a LICOR 193-SA Quantum Sensor: 100%, 55%, 27%, 11%, 5%, and 2%. Duplicate productivity samples were estimated for each light level by 24-hour simulated *in situ* incubations with ^{14}C-bicarbonate (Vernet *et al.* 1996). The temperature of the incubations was maintained using the seawater intake system both at Palmer Station and during the cruise. For Palmer Station, the seawater is collected from the harbour near the station and is representative of the Standard Seawater Temperature (SST) within the near shore sampling grid. The SSTs at stations B and E are quite similar over the course of the season (mean standard deviation between stations of 0.30°C) and demonstrate a general warming trend over the course of the season. For the cruise data, the temperature of the incubations is that of the water through which the ship is travelling and may not always represent the SST from which the phytoplankton were collected, but is accurate to +/-2°C.

Total chlorophyll was quantified from filtered samples (Millipore HA filters) using standard fluorometric techniques on a digital Turner Fluorometer (Smith *et al.* 1981). Chlorophyll *a* (chl *a*) was calculated by subtracting phaeopigment concentration determined by sample acidification. All samples were analysed within 2–3 days of collection. Additional algal pigments were determined by using high-performance liquid chromatography with a gradient system and a reverse-phase C-18 column (Kozlowski *et al.* 1995). The taxonomic composition was determined by analysing the ratio of specific pigments to chl *a*. The concentration of fucoxanthin (Fuco) was used to indicate diatoms, alloxanthin (Allo) for cryptophytes, chlorophyll *b* (chl *b*) for green algae, and the sum of 19'-hexanoyloxyfucoxanthin and 19'- butanoyloxyfucoxanthin for chromophytes (Hex + But). Multiple regression was performed on the pigment concentrations (mg m^{-3}) of the surface waters (depths corresponding to 100% and 55% light levels) against chl *a* concentrations for both 1994–95 and 1995–96 seasons (Bidigare *et al.* 1986, Gieskes *et al.* 1988, Claustre *et al.* 1997). The equation used was:

$$\text{chl}\,(a) = 1.58Fuco + 3.28Allo + 0.56(Hex + But) + 2.33\text{chl}\,b \quad (1)$$

We assumed that multicolinearity of the input variables was negligible. This method only approximates dominant taxonomic groups in a phytoplankton assemblage.

We also compiled a set of historical chl *a* and primary productivity data collected primarily from the Antarctic Peninsula region from 1972–90 (Smith *et al.* 1996a, Behrenfeld & Falkowski 1997b). The historical data-set consists of a relatively large number of chl *a* observations ($n = 438$) and a smaller subset of both chl *a* and primary productivity with sufficient ancillary data to generate depth-integrated values ($n = 86$) within the euphotic zone. When the euphotic depth (Z_{eu}) was not provided for the data, we estimated Z_{eu} to the 2% light level using a relationship developed from the LTER data ($r^2 = 0.37$, $P < 0.01$):

$$Z_{eu} = 48.8\,C_0^{-0.36} \quad (2)$$

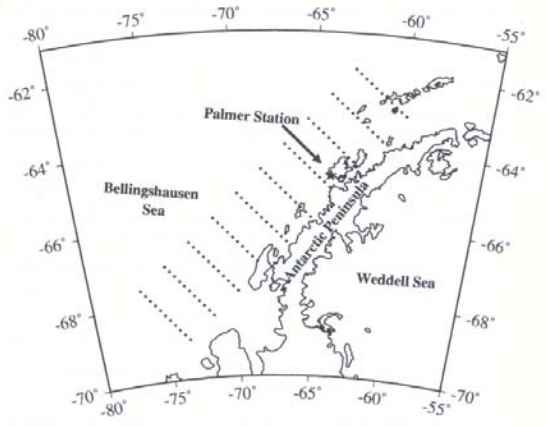

Fig. 1. Location of Palmer Station and the LTER grid in reference to the Antarctic Peninsula.

The reliability of historical phytoplankton production data is of some concern, especially data collected prior to the mid 1980s when "clean" techniques were not in use. Martin *et al.* (1990) suggests that clean techniques are most important in open oligotrophic regions where iron is limiting (Martin *et al.* 1990). As most of the data we discuss was obtained in coastal waters where iron is not considered to be limiting, we would expect little difference between "clean" and "classical" techniques for the data presented here. These historical data are discussed in detail by Smith *et al.* (1996a).

Downwelling photosynthetically available radiation (400–700 nm) at the ocean surface, $E_d(0^+, 400–700)$, is estimated for each 24-hour incubation period using measurements taken from a spectroradiometer located at Palmer Station (Booth *et al.* 1995). This instrument provided hourly measurements of downwelling light integrated from 400–600 nm. Irradiance is then extrapolated out to 700 nm using a site-specific modelled relationship between irradiance integrals from 400–600 vs 400–700 nm:

$$E_d(0^+,400–700) = 1.42E_d(0^+,400–600) - 1.15 \quad (3)$$

This relationship has been derived using the atmospheric radiative transfer model SBDart (Gautier & Frouin 1992) with different modelled cloud layers, surface albedos, and solar zenith angles. These estimates of $E_d(0^+)$ are highly correlated with measurements of scalar $E_0(0^+)$ made using a Biospherical Instrument QSR250 located near the primary productivity incubators at Palmer Station ($r^2 = 0.82$; data not shown). For the ship incubations, this correlation was used to estimate $E_d(0^+, 400–700)$ from the scalar measurements of $E_0(0^+)$ made from a QSR250 onboard ship.

A method of evaluating the relationship between rates of primary productivity and the *in situ* irradiance (P vs E) is to treat the water column as a compound photosynthetic system and estimate P vs E parameters for the entire water column (Talling 1957, Behrenfeld & Falkowski 1997b). This approach is different from P vs E curves measured under conditions of constant irradiance, because the productivity for each sample is measured under irradiance conditions that can vary from light-limiting to photoinhibiting over the course of an incubation. These in-water P vs E curves have different physiological interpretations and terminology than the short-term P vs E curves (see Table I for terminology used throughout this paper). Vollenwieder (1966) and, more recently, Behrenfeld & Falkowski (1997b) have discussed the differences between parameters used in time-integrated models and photosynthesis-irradiance variables (Vollenwieder 1966, Behrenfeld & Falkowski 1997a). Measured values of productivity normalized by chl, P^B_z, are normalized to the chl-specific maximum rate of water column photosynthesis, P^B_{opt}, and modelled as a function of the daily irradiance using the P vs E equation (Platt & Sathyendranath 1988, Behrenfeld & Falkowski 1997b):

$$\frac{P^B_\zeta}{P^B_{opt}} = \frac{P^B_s}{P^B_{opt}}\left(1 - \exp(-\frac{E_\zeta}{E_{\max}})\right)\exp(-\beta\ E_\zeta) \quad (4)$$

where E_ζ is the irradiance at a given optical depth, E_{max} is the irradiance at the inflection point between light limitation and light saturation in the absence of photoinhibition, P^B_s is the

Table I. Terminology.

Parameter	Units	Description
chl *a*	chl	chlorophyll *a*
C_z	mg chl	measured chl at depth *z*
C_{eu}	mg chl m^{-2}	water column chl integrated to euphotic depth
C_{50}	mg chl m^{-2}	water column chl integrated to 50 m
C_0	mg chl m^{-3}	surface chl
PP_{eu}	mg C m^{-2} d^{-1}	water column primary productivity integrated to euphotic depth
Z_{eu}	m	euphotic depth
D	h	photoperiod
$E_d(0^+)$	Ein m^{-2} d^{-1}	daily downwelling irradiance (400–700 nm) incident upon the sea surface
$E_0(0^+)$	Ein m^{-2} d^{-1}	scalar irradiance (400–700 nm) incident upon the sea surface
E_ζ	Ein m^{-2} d^{-1}	daily downwelling irradiance at optical depth, ζ
E_{max}	Ein m^{-2} d^{-1}	daily downwelling irradiance at the inflection between light limitation & light saturation in absence of photoinhibition
SST	°C	sea surface temperature
P^B_z	mg C mg chl^{-1} d^{-1}	chl-normalized primary productivity by discrete depth
P^B_ζ	mg C mg chl^{-1} d^{-1}	chl-normalized primary productivity by optical depth
P^B_{opt}	mg C mg chl^{-1} h^{-1}	chl-normalized maximum rate of photosynthesis normalized by photoperiod for the water column
P^B_s	mg C mg chl^{-1} h^{-1}	chl-normalized maximum rate of photosynthesis normalized by photoperiod in absence of photoinhibition for water column
α	mg C mg chl^{-1} h^{-1} (μEin m^{-2} s^{-1})$^{-1}$	chl-specific rate of light-limited photosynthesis in the water column
β_d	(μEin m^{-2} s^{-1})$^{-1}$	Photoinhibition slope for the water column
E^*_K	μEin m^{-2} s^{-1}	saturation parameter of photosynthesis for the water column
F	(dimensionless)	ratio of mean chl-normalized productivity in the water column to P^B_{opt}
ψ	mg C m^{-2} d^{-1} (mg chl m^{-2} Ein m^{-2} d^{-1})$^{-1}$	light utilization index

maximum normalized productivity in the absence of photoinhibition, and β_d is the variable slope for surface photoinhibition. Daily production was converted to hourly production using the photoperiod. Equation 4 is the same as Behrenfeld & Falkowski (1997b), but explicitly contains the factor of P^B_s to P^B_{opt} required for proper scaling of the model. The observed patterns of P^B_z were fit to Eq. 4 using a Gauss-Newton non-linear curve fitting routine with Levenburg-Marquardt modifications (Zimmerman *et al.* 1987). Model II regression techniques (Laws & Archie 1981) were utilized throughout this manuscript in cases where both the independent and the dependent variable were subject to natural variability.

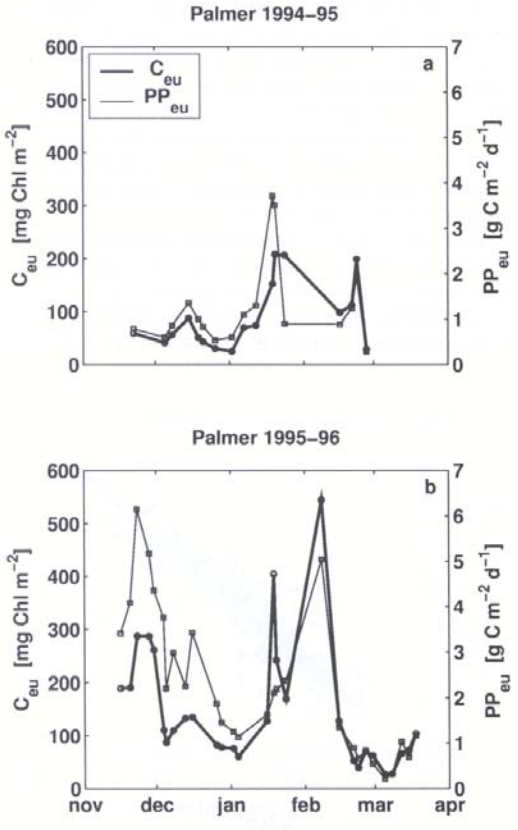

Fig. 2. Distribution of water column integrated chl *a* and water column integrated daily primary production for **a.** 1994–95 season, **b.** 1995–96 season. The data from stations B and E have been averaged. The mean standard deviation between these stations is 25 mg chl m^{-2} for C_{eu} and 0.35 g C m^{-2} d^{-1} for PP_{eu}.

Results and discussion

Distribution of chlorophyll a and primary production

Water column integrated values for both chl *a* (C_{eu}) and daily primary production (PP_{eu}) over the 1994–95 and 1995–96 field seasons at the inshore stations B and E are shown in Fig. 2. As shown, chl *a* and PP_{eu} are highly correlated throughout the season. Both biomass and productivity show significant interannual variability with 1995–96 levels being higher than the 1994–95 levels. For the 1994–95 field season at Palmer Station, the median C_{eu} is 69 mg chl m^{-2} and ranges from 22 to 280 mg chl m^{-2}. The median PP_{eu} is 1.0 g C m^{-2} d^{-1} and ranges from 0.3 to over 4 g C m^{-2} d^{-1}. For 1995–96, the median C_{eu} is 101 mg chl m^{-2} and ranges from 20 up to 600 mg chl m^{-2} and the median PP_{eu} is 1.5 g C m^{-2} d^{-1} and ranges from 0.13 to over 6 g C m^{-2} d^{-1}. Because biomass and productivity are lognormally distributed and blooms occur infrequently, the median values for C_{eu} and PP_{eu} are significantly lower than the mean values. Figure 2 also shows that both years of data typically display two to three phytoplankton blooms during each growing season. One bloom generally occurs in January with additional blooms occurring in fall and/or spring. These blooms persist for approximately one to two weeks. This general pattern was also was observed in earlier time series data from these stations (Moline & Prezelin 1996).

Vertical profiles of chl, productivity, and chl-normalized productivity (P^B_z) for the Palmer nearshore and offshore LTER data are shown in Fig. 3a–c. The profiles have been normalized to the mean value in the profile and the shaded area represents one standard deviation from the mean. In general, the vertical structure of all three variables shows a maxima at or near the surface and a gradual decrease with depth. Also, the vertical structure of chl (Fig. 3a) is fairly uniform within the top two optical depths of the water column. Thus, the highest concentrations of chl are generally well within the layer of water that can be remotely sensed by an ocean colour satellite (i.e. one optical depth which is shown by the dotted lines in Fig. 3) (Gordon & McGluney 1975, Smith 1981). As the vertical structure of chl within the water column is fairly consistent amongst all profile data, the surface concentrations of chl (C_0) explains nearly 84% of the integrated water column chl variance with a log–log regression (Fig. 4), such that:

$$C_{eu} = 42.7C_0^{-0.66} \qquad (5a)$$

This relationship is nearly identical both to that determined with the historical data and estimated using Eq. 2. Lines 2 and 3 on Fig. 4 show almost identical relationships to Eq. 5a. However, these relationships differ significantly from that developed previously for high latitudes (Morel & Berthon 1989), which underestimates integrated chl (Fig. 4, line 5).

We also compared these results to relationships developed using chlorophyll integrated to 50 m, C_{50}, and found them also to be very similar (Holm-Hansen & Mitchell 1991). As

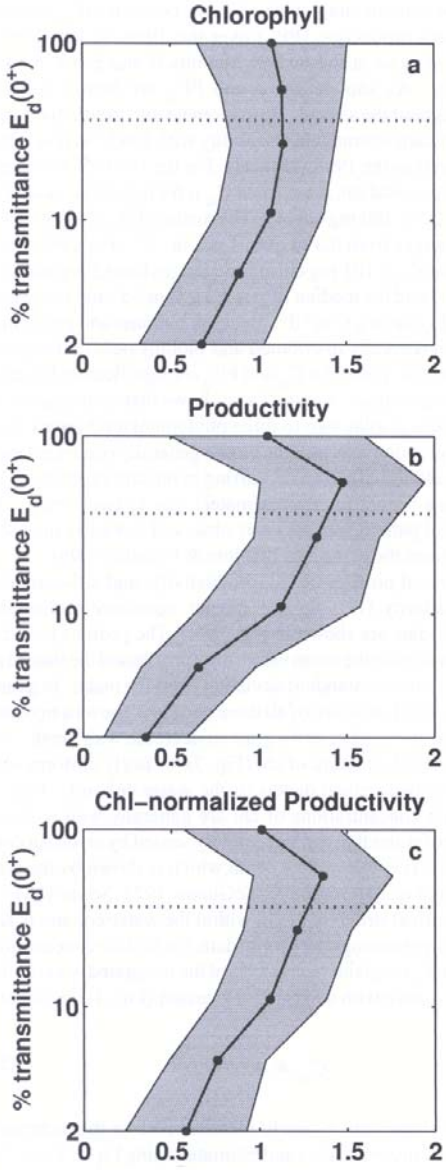

Fig. 3. Mean vertical profiles of 177 stations from the Palmer nearshore and offshore area. Data have been normalized by the average concentration within the euphotic zone and are unitless. Shaded area represents one standard deviation from the mean and the dotted line represents the penetration depth of an ocean colour sensor (i.e. one optical depth). **a.** chl *a*, **b.** productivity, **c.** chl-normalized productivity.

expected, C_{50} underestimates C_{eu} for low chl concentrations and overestimates C_{eu} for high chl concentrations (data not shown), such that:

$$C_{50} = 2.17 C_{eu}^{0.75} \quad (5b)$$

While chl concentrations can remain high at depths beneath the euphotic zone (Holm-Hansen & Mitchell 1991), generally the highest biomass concentrations are found near the surface where most of the primary production occurs. For these waters, the euphotic zone is generally found within the wind mixed layer, which is consistent with a more uniform vertical profile of chl.

Primary productivity generally peaks at an optical depth of 0.6 or when approximately 50–55% of the incoming $E_d(0^+)$ has been attenuated (Fig. 3b). Hence, the rates of primary production at the surface appear to be photoinhibited when compared to the rates at the 55% light level. However, this peak generally occurs within the top optical depth of the water column, well within the depth from which a satellite signal can be received. The presence of a C_0 and primary productivity maxima is consistent with past findings in this region of the Southern Ocean (Smith *et al.* 1996a). The daily profile of PP_{eu} decreases more rapidly with depth than either the chl or chl-normalized productivity profiles.

When productivity is normalized to chl, photoperiod and optical depth (P^B_z), the vertical profile still exhibits the same basic shape as the productivity profile (Fig. 3c). When compared to the vertical structure of data collected from all of world's oceans (Behrenfeld & Falkowski 1997b), the actual

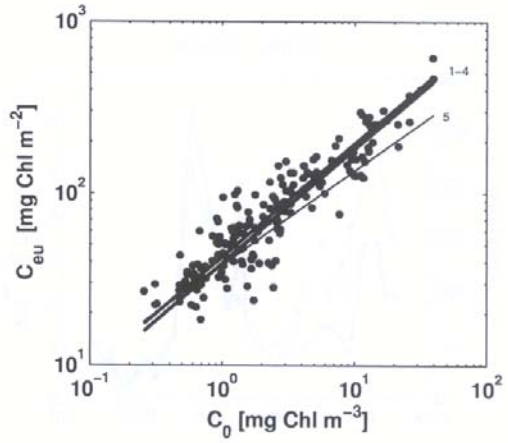

Fig. 4. Relationship between the surface chl concentrations (C_0) and the water-column integrated chl concentration (C_{eu}). Numbered lines represent: 1. these data $C_{eu} = 42.7\ C_0^{0.66}$ (n = 185, $r^2 = 0.84$), 2. historic data, 3. C_0 x Z_{eu} (Eq. 2), 4. Holm-Hansen & Mitchell (1991) using Eq. 5b to convert C_{50} to C_{eu}, 5. Morel & Berthon (1989) for high latitudes.

profiles of normalized productivity for the Palmer data are both much more uniform with depth and of a lower magnitude than for the global data (Fig. 5a). The shaded region in Fig. 5a represents the normalized productivity data used in the global productivity algorithm developed by Behrenfeld & Falkowski (1997a, Fig. 1b). As shown, the P^B_z profiles for the Antarctic data peak around 1 mg C mg chl^{-1} hr^{-1}, which is significantly lower than for other oceanic waters. Both the shape and the magnitude of the LTER data shown in Fig. 5a have significant implications for modelling primary productivity in Antarctic waters.

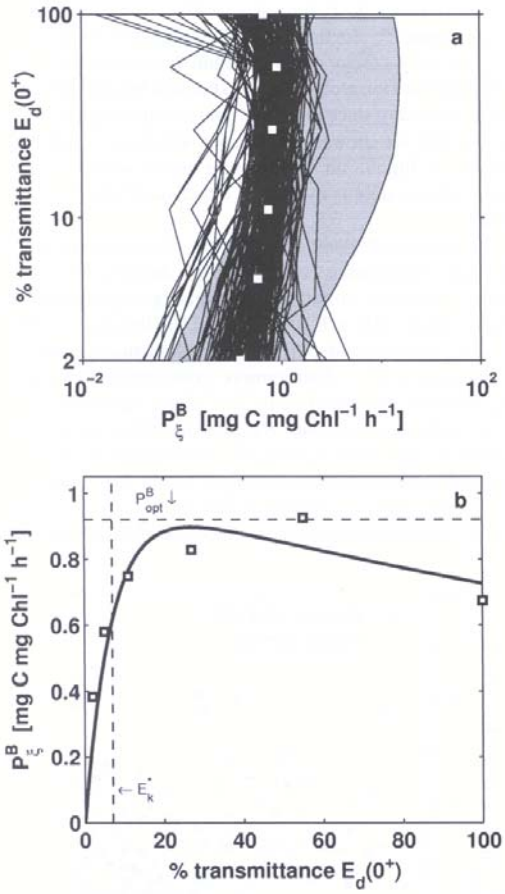

Fig. 5. a. Vertical profiles of chl-normalized productivity for the Antarctic data. Shaded region represents the data used in the global productivity algorithm developed by Behrenfeld & Falkowski (1997a, fig. 1b, p. 5). White squares represent the median for the Antarctic data. **b.** Datapoints are the median vertical profile from Fig. 5a plotted against the corresponding percent transmission of incident light. These are time-integrated P vs E parameters representing the entire water column and the line represents the fit to the data using Eq. 4.

If the median of the Palmer nearshore and offshore chl-normalized productivity data from Fig. 5a (white squares) are plotted against the corresponding percent transmission of incident irradiance, this relatively uniform vertical structure can be transformed into a type of time-integrated P vs E curve representing the water column. As shown in Fig. 5b, this curve has a steep slope indicative of a relatively low E_k*, rising to a P^B_{opt} above 0.9 mg C mg chl^{-1} h^{-1}, followed by a gradual decreasing slope indicative of photoinhibition. E_k* is defined as the irradiance at the inflection point between light limitation and light saturation observed from measured P^B_z in the water column. On average, E_k* occurs when approximately 7% of the surface light remains ($E_k^*/E_0 = 0.07$). Because E_k* generally occurs deep within the water column, much of the daily production occurs at irradiance levels above E_k*. In other words, chl-normalized productivity does not decrease as rapidly with depth as it does for phytoplankton in other regions of the world. Having both a low E_k* and P^B_{opt} is characteristic of phytoplankton that are adapted to low-light conditions and/or low water temperatures and is consistent with past studies from this region (Smith & Sakshaug 1990, Holm-Hansen & Mitchell 1991, Smith *et al.* 1996b).

For these Antarctic waters, the median P^B_{opt} for our data set is 1.09 mg C mg chl^{-1} h^{-1}, with P^B_{opt} varying by nearly a factor of seven over the course of a season. Figure 6 shows a time series of P^B_{opt} as it varies over the course of the 1994–95 and 1995–96 field seasons, respectively. The P^B_{opt} measured for stations B and E have been averaged (shading represents one standard deviation from the mean) and are highly variable over the course of a season. As shown in Fig. 6, no obvious seasonal trend is evident in P^B_{opt} for the two field seasons. For 1994–95, P^B_{opt} approaches 1.5 in late December to early January and is less than 1 both before and after this period. For 1995–96, P^B_{opt} is high (approaching 2) from November through December and then closer to 1 throughout the remainder of the year. Additionally, the variability in P^B_{opt} over the course of a season does not appear to follow the corresponding variability in productivity (Fig. 2b), nor does it follow the seasonal variability in water temperature, which shows a general warming trend throughout the season (Fig. 6). For example, P^B_{opt} is low for the 1994–95 mid-January phytoplankton bloom, relatively high for the early 1995–96 bloom, and only average for the late 1995–96 bloom. Both the lower magnitude of P^B_{opt} and the more uniform vertical structure of normalized productivity are discussed below in the context of primary productivity models.

Environmental influence on photoadaptation

Behrenfeld & Falkowski (1997a, 1997b) have shown that model performance in estimating depth-integrated primary productivity is critically dependent on the ability to accurately represent the space/time variability of the photoadaptive parameter, P^B_{opt}. They suggest that model improvement will

depend upon a mechanistic understanding of how environmental variability affects the physiological state of phytoplankton assemblages. While chl explains most of the variability in PP_{eu}, variability in P^B_{opt} and the vertical distribution of the chl-normalized productivity can also significantly impact estimates of PP_{eu}. Here we seek to identify environmental variables that may explain the variability in these parameters and emphasize those that may be remotely sensed and could potentially allow more accurate modelling of PP_{eu} from remotely sensed biomass.

As photosynthesis is the result of an enzymatically controlled rate process, it is sensitive to ocean temperatures (Tilzer *et al.* 1986). Recent estimates of global ocean primary production have used sea surface temperature (SST) to predict the magnitude of a photoadaptive variable (Antoine & Morel 1996, Behrenfeld & Falkowski 1997b). Such an approach is advantageous because SST can be determined remotely and used to delimit biogeochemical provinces for global modelling. Antarctic phytoplankton south of the Polar Front live in the coldest surface waters, with temperatures from nearly -2 to 2°C. While some thermal adaptation may occur, P^B_{opt} ranges from 0.4–3 mg C mg chl^{-1} h^{-1}, which is in the range expected for a cold water system (Smith *et al.* 1996b). However, within this limited temperature range, no significant relationship appears to exist between SST and P^B_{opt} for our nearshore and offshore data (Figs 6 & 7). The polynomial model described by Behrenfeld & Falkowski (1997a) (Fig. 7) tends to overestimate P^B_{opt} for the temperatures between 0 and 2°C and P^B_{opt} varies by a factor of seven within this temperature range. The poor fit of the global model to this low temperature range is not surprising since this is the temperature range where the global data set showed the greatest variability. Indeed, as shown in Fig. 7, no temperature trend within this low temperature range is evident in either our Palmer or cruise data.

We also investigated several other environmental factors that may influence the variability in P^B_{opt} and may be remotely sensed. However, no single parameter or group of parameters that we analysed (e.g. $E_d(0^+)$, SST, chl, daylength, cloud ratio, salinity, mixed layer depth) produces a statistically significant relationship to P^B_{opt}. Furthermore, considering the variables together only explained up to 20% of the variability in P^B_{opt} using multiple regression. We considered that variable light histories might influence the P^B_{opt} of the phytoplankton, but found no relationship between $E_d(0^+)$ from days prior to the incubation. No discernible relationship was found between Antarctic phytoplankton blooms and sea surface salinity based

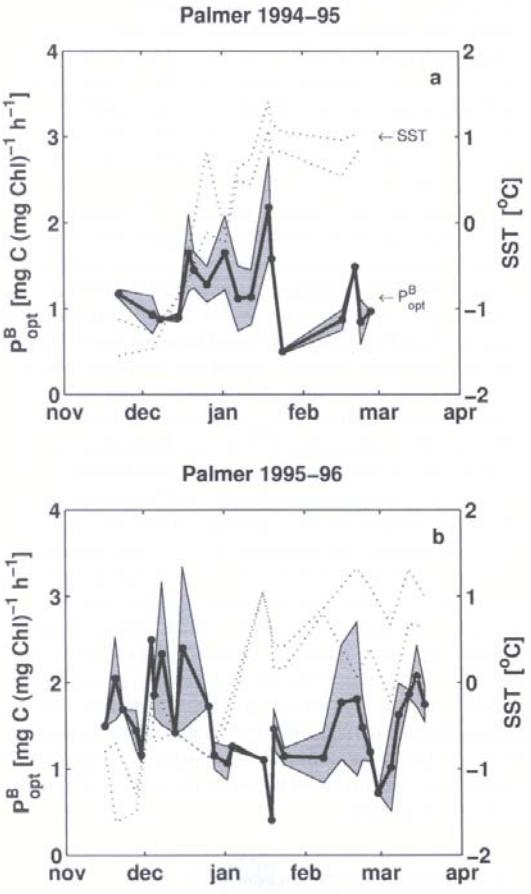

Fig. 6. Measured estimates of P^B_{opt} over the field season averaged for stations B and E and shading represents one standard deviation from the mean for the two stations. Dotted line represents the SST of both stations B and E for each season. **a.** 1994–95 season, **b.** 1995–96 season.

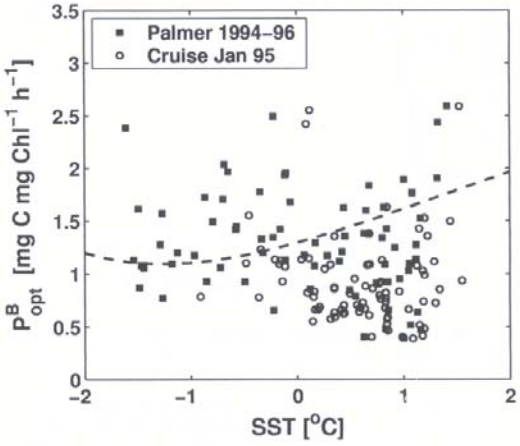

Fig. 7. Measured estimates of P^B_{opt} vs sea surface temperature. The dashed line is that corresponding to Behrenfeld & Falkowski (1997a, Eq. 11).

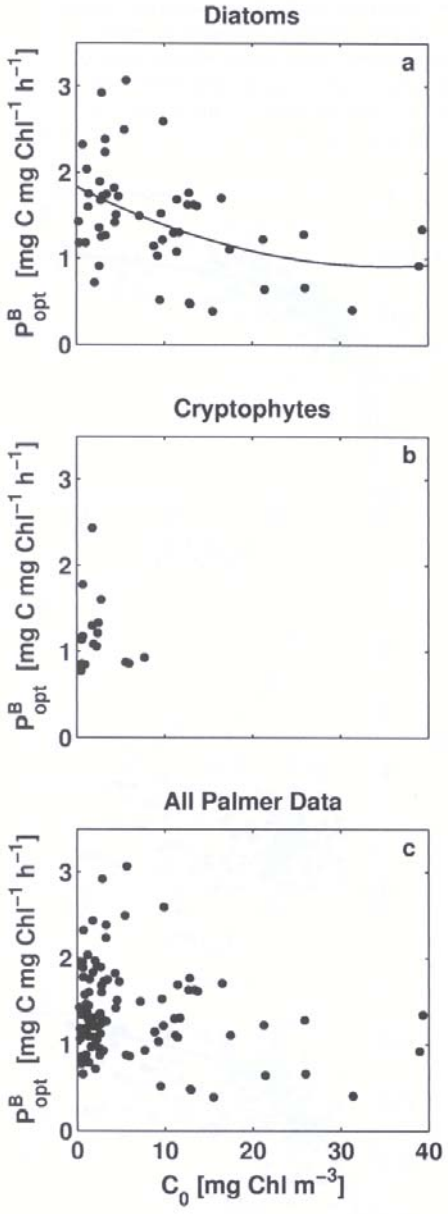

Fig. 8. Comparison of P^B_{opt} [mg C mg chl^{-1} h^{-1}] for nearshore Palmer data for when the water column is **a.** > 60% diatoms, **b.** > 60% cryptophytes, **c.** all Palmer data. The line for the diatoms (Fig. 8a) is significant ($P < 0.01$, $r^2 = 0.14$). No significant trend was evident in the other two panels.

upon water column stability from melting sea ice and coastal glaciers, but no discernable relationship was found. Past findings from this region also found that photosynthesis-irradiance parameters were poorly correlated to physical forcing and nutrient regimes (Moline *et al.* 1998).

Because different species of phytoplankton in this region have different carbon to chl ratios (C:chl) and pigment-specific absorption coefficients (Brody *et al.* 1992), some of the variability in P^B_{opt} could be due to the presence of different bloom-forming phytoplankton (e.g. diatoms vs cryptophytes). Figure 8a & b show P^B_{opt} for sampling events from the inshore Palmer data when the phytoplankton were mainly diatoms (high in fucoxanthin/chl ratio) and mainly cryptophytes (high in alloxanthin/chl ratio), respectively. Figure 8c shows the relationship between P^B_{opt} and C_0 for all of the Palmer data regardless of taxonomic composition. As shown, cryptophytes are estimated to be the dominant taxa (> 60%) in the water column less frequently than diatoms. Moreover, the very large blooms (C_0 > 10 mg chl m^{-3}) tend be diatom blooms. Cryptophytes cover a smaller range in P^B_{opt} and have a median value of 1.20 and a standard deviation of 0.47 mg C mg chl^{-1} h^{-1}. The range in P^B_{opt} is greater for the diatoms, which vary from 0.9–2.44 mg C mg chl^{-1} h^{-1}, but there is no statistically significant difference between P^B_{opt} for the two taxa. In addition to the more numerous diatom blooms, another reason for the larger range in P^B_{opt} could be because different species of diatoms can be either larger or smaller than cryptophytes, which may contribute to different internal ratios of C:chl. Over the course of a season, the dominant diatom taxa at Palmer Station can vary to include both large and small diatoms, which will similarly cause variance in P^B_{opt}. Such a difference may not be as evident from data collected over a restricted time period (Brody *et al.* 1992). While P^B_{opt} tends to decrease with increasing C_0 on all three panels (Fig. 8a–c), the concentration of C_0 is not a good predictor of P^B_{opt} because P^B_{opt} still varies by a factor of seven for low chl concentrations.

Another parameter that also plays a role in modelling primary productivity is the relationship of P^B_{opt} to the mean chl-normalized productivity (P^B_Z). The function F is used to describe the loss in potential photosynthesis due to light limitation and photoinhibition and can be estimated as the ratio of the mean P^B_Z with depth versus P^B_{opt} (Wright 1959, Behrenfeld & Falkowski 1997a). While F does not explain much of the variability in PP_{eu} (< 2%), F is a linear term in the model and hence is important in determining the overall magnitude of primary production. In the absence of photoinhibition, F should demonstrate an irradiance-dependence such that the F function is lower when $E_d(0^+)$ is low (more of the water column is light-limited), and F approaches a maximum when $E_d(0^+)$ is high (more of the water column is light-saturated) (Behrenfeld & Falkowski 1997a). Because the vertical structure of chl-normalized productivity for these Antarctic data are much more uniform with depth (Fig. 5), the phytoplankton are operating close to P^B_{opt} throughout much of the water column and consequently F is

higher (mean of 0.64) for these Antarctic data than the mean of 0.55 estimated for the global data-set (Behrenfeld & Falkowski 1997a).

The F parameter is commonly compared to the ratio of $E_d(0^+)$ to E_K^*, the light intensity corresponding to the intersection between the light-limited slope of primary productivity in the water column and P^B_{opt} (Fig. 9a). While our F is higher than that derived from the global data-set (Behrenfeld & Falkowski 1997a), it is lower than the theoretical derivation of F assuming no photoinhibition (Talling 1957). Because E_K^* is low and often occurs near the bottom of the euphotic zone, the range of $E_d(0^+)/E_K^*$ extends to much higher values than previously published (i.e. > 25). The tight correlation shown in Fig 9a is expected because the vertical profile of chl-normalized production, and thereby F, can be derived from the photosynthesis-irradiance parameters used to describe the water column (i.e. E_K^*). However, this relationship (Fig. 9a) cannot be used to model F because either E_K^* or the ratio $E_d(0^+)/E_K^*$ must be known *a priori*. As shown in Fig. 9b, E_K^* is not readily estimated from $E_d(0^+)$ for these data. E_K^* varies between 0 and 8 Ein m^{-2} d^{-1} and displays little relationship to $E_d(0^+)$. The dashed line on Fig. 9b was developed for the global data-set (Behrenfeld & Falkowski 1997a) and does not fit these data. It is possible that this lack of correlation could be due to the extremely variable light environment to which these phytoplankton are exposed.

The relationship between F and $E_d(0^+)$ (Fig. 9c), however, is statistically significant ($P < 0.01$), although it explains little of the variability in F ($r^2 = 0.23$). We derive the following empirical relationship:

$$F = \frac{E_d(0^+)}{E_d(0^+) + 11.77} \tag{6}$$

Optimization of primary productivity model

Behrenfeld & Falkowski (1997a) have shown that, in general, depth-integrated models can be reduced to a relationship describing depth-integrated primary productivity from phytoplankton biomass (C_{cu}), a photoadaptive variable (P^B_{opt}), an irradiance-dependent function (F), and daylength (D). Further, they show that depth-integrated productivity models are fundamentally synonymous and most of the variability in estimating primary productivity involved differences in the input biomass and estimate of photoadaptive variability. Hence, more complex primary productivity models, involving additional levels of integration (i.e. time, wavelength, depth), are not likely to explain significantly more of the variability in primary productivity until the photoadaptive variability is better characterized. As discussed above, in investigating the

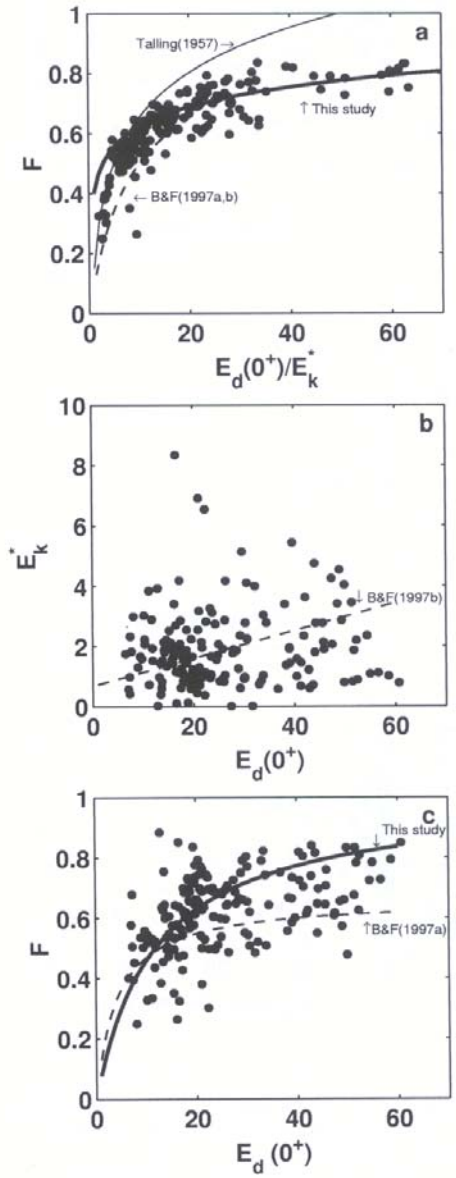

Fig. 9. a. F, which represents the mean chl-normalized productivity with depth vs P^B_{opt}, as a function of $E_d(0^+)/E_K^*$. The thick line represents the best fit to this data. The thin line represents the fit by Talling (1997). Dashed line represents the fit using eqs. 30 & 31 from Behrenfeld & Falkowski (1997b). **b.** Comparison of the surface irradiance $E_d(0^+)$ shown as a function of E_K^*. Dashed line represents the fit using eq. 31 from Behrenfeld & Falkowski (1997b). **c.** Comparison of the surface irradiance ($E_d(0^+)$ and the function F. Solid line represent fit using Eq. 6 ($r^2 = 0.23$, $P < 0.01$). Dashed line represents the fit to the global data set (Behrenfeld & Falkowski 1997b, eq. 30).

environmental influences on photoadaptive variability, we found no consistent predictor or set of predictors that could be used to reliably predict P^B_{opt} for these Antarctic waters.

We utilize the standard depth-integrated model structure (Behrenfeld & Falkowski 1997b) and tune the model to fit the Antarctic data (both the cruise data and the inshore Palmer data):

$$PP_{eu} = P^{\beta}_{opt} D C_0 Z_{eu} F \quad (7)$$

For our parameterization of the model, we use F estimated from $E_d(0^+)$ (Eq. 6), the median value for P^B_{opt} (1.09 mg C mg chl^{-1} h^{-1}), and Z_{eu} derived from C_0 (Eq. 2). Using measured values of C_0 and $E_d(0^+)$, this model explains nearly 72% of the variability in the data on a log scale and closely follows a 1:1 correspondence line (Fig. 10a). If we further simplify the model and use a constant F of 0.64, the model only loses 5% of predictive capability. Because the median P^B_{opt} (1.01 mg C mg chl^{-1} h^{-1}) for the large blooms is very similar to the median P^B_{opt} (1.09 mg C mg chl^{-1} h^{-1}) from all nearshore and offshore LTER data, our model is more effective for days with extremely high PP_{eu}. This is important because a significant fraction of seasonal production occurs under high bloom conditions.

In addition to applying this model to the LTER data from which it was derived, we also applied it to historic primary productivity data from the Antarctic (Fig. 10b). The historic data shown here were collected in the Antarctic Peninsula region and South Indian Sector of the Southern Ocean from 1972–90 (Smith *et al.* 1996a). When irradiance data was not available within this data set, a constant F of 0.64 was used in the model instead of Eq. 6. Even without irradiance data, the model performed just as well on the historic data as on the LTER data and explained 73% of the variability in PP_{eu}. Moreover, we find nearly a 1:1 correspondence between the measured and modelled data (m = 1.02, b = -0.11). It will be of interest to test the model for other regions of the Southern Ocean.

Table II presents a comparison of our model parameterization (Eq. 7) with various published algorithms. The VGPM model developed for the global oceans (Behrenfeld & Falkowski 1997b) in its original form explains approximately 61% of the variability for the Antarctic data and tends to overestimate productivity for low PP_{eu} and underestimate for high PP_{eu}. In fact, for these waters it explains less of the variability in PP_{eu} than a simple regression on C_0. We believe this is primarily due to three sources of error when applying the model to Antarctic waters:

1) the equation relating P^B_{opt} and SST overpredicts P^B_{opt} at SST > 1°C (Fig. 7),
2) the F function is generally underestimated (Fig. 9), and
3) the relationship (Morel & Berthon 1989) used to estimate Z_{eu} generally underestimates C_{eu} (Fig. 4).

Using measured C_0 and a constant light utilization index ψ (Morel 1991) the Laboratoire de Physique et Chimie Marines (LPCM) model (Antoine *et al.* 1996) explains 69% of the variability in the data. For these data, ψ (which is related to the water column averaged functional absorption cross-section for photosynthetic carbon fixation ψ^*) varies from 0.2 to 2 and has a median value of 0.56 mg C m^{-2} d^{-1} (mg chl m^{-2} Ein m^{-2} d^{-1})$^{-1}$. This is higher than that estimated for temperate waters and near the average ψ determined previously for this region (Claustre *et al.* 1997). The parameter ψ can be related to P^B_{opt}

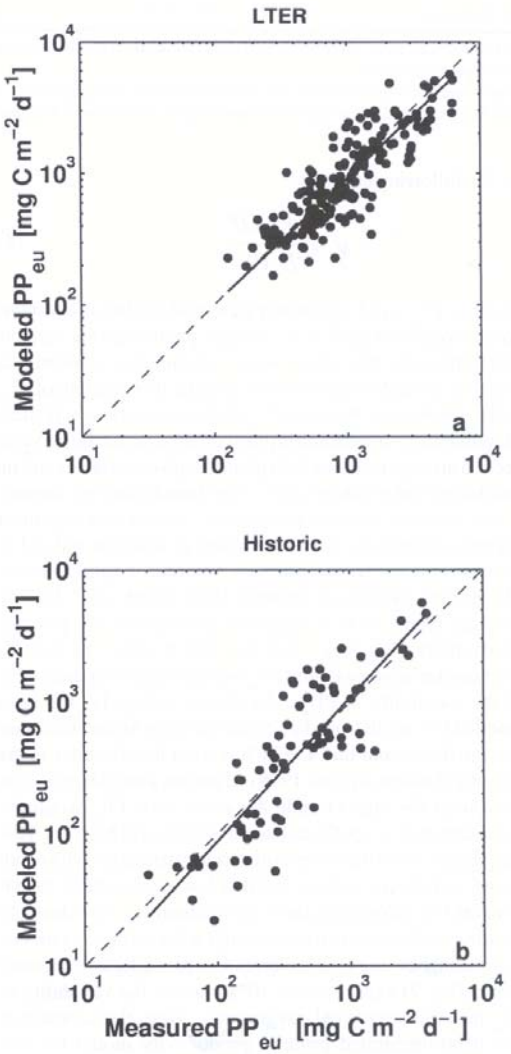

Fig. 10. Measured primary productivity vs modelled primary productivity using Eq. 7 for the **a.** LTER data (n = 186, r^2 = 0.72, m = 0.96), **b.** Historic data (Smith *et al.* 1996) (n = 82, r^2 = 0.73, m = 1.09).

Table II. Statistical comparison of measured vs modelled daily primary production.

Model	Formulation	Regression statistics[1]		Source
		r^2	m,b	
Antarctic Model[2]	$PP_{eu} = P^B_{opt}\ D\ Z_{eu}\ C_0\ F$	0.72	0.96, 0.1	[Eq. 6]
C_θ	*$PP_{eu} = C_\theta$*	*0.62*		
Z_{eu}	*$PP_{eu} = Z_{eu}$*	*0.28*		
P^B_{opt}	*$PP_{eu} = P^B_{opt}$*	*0.18*		
F	*$PP_{eu} = F$*	*0.02*[3]		
D	*$PP_{eu} = D$*	*0.02*		
VGPM Model	$PP_{eu} = P^B_{opt}\ D\ Z_{eu}\ C_0\ F$	0.61	0.92, 0.2	[Behrenfeld & Falkowski 1997a]
LPCM Model	$PP_{eu} = \psi\ Z_{eu}\ C_0\ E_d(0^+)$	0.69	1.06, -0.2	[Antoine *et al.* 1996]
chl Regression	$PP_{eu} = 513\ C_0^{0.725}$	0.62	1.0, 0	[Fig. 10]

[1]log-linear regressions were performed using Model II regression techniques (Laws & Archie 1981), where r^2 = correlation coefficient, m = slope, b = intercept of regression.
[2]Each component of this model was individually regressed against PP_{eu}, as presented in italics below.
[3]For this parameter, linear regression had a higher correlation to PP_{eu} than a log-linear regression.

by the following equation:

$$\psi = \frac{P^B_{opt}\, DF}{E_d(0^+)} \qquad (8)$$

Because P^B_{opt} and F can nearly be approximated as constants for this region (Figs 7 & 9), using a photoadaptive variable that represents the entire water column (ψ) is nearly as effective as modelling with more specific formulations of P^B_{opt} and F. Moreover, because P^B_{opt} and ψ are so closely related, the possible environmental influences discussed in the previous section are applicable to both photoadaptive variables and no environmental predictors of ψ were found (data not shown).

The simplest primary productivity model is a log-linear regression between rates of primary production and chl *a*. Consistent with earlier reports for Antarctic waters (Minas & Minas 1992, Moline & Prezelin 1996, Smith *et al.* 1996a), biomass seems to be a relatively good proxy for primary productivity (Fig. 11). For the LTER data, the best-fit relationship between C_0 and PP_{eu} explains approximately 62% of the variability in PP_{eu}. As shown in Fig. 11, the lines labelled 1–3 are all from data collected in the Antarctic and are quite distinct from line 4, which is from low latitudes in the Atlantic (Falkowski *et al.* 1998). If the low latitude regression were used for high latitude Antarctic data, PP_{eu} would be overestimated at low C_0 and underestimated at high C_0. This is probably due to the more uniform chl distribution with depth found in Antarctic waters. If chl is low at the surface, then it remains low throughout the water column (i.e. few deep chl maxima) and similarly if chl *a* is high at the surface, it remains high throughout the water column. Our tuned depth-integrated model (Eq. 7) explains only 10% more of the variability in PP_{eu} than this simple chl *a* regression. Thus, the accuracy of any depth-integrated primary productivity model for this region is primarily dependent on determining the appropriate biomass concentration and the correct relationship between PP_{eu} and C_{eu}.

Conclusions

Using time series data of chlorophyll and daily net primary production measured in the coastal waters of Palmer Station, Antarctic Peninsula, we have evaluated models to estimate photoadaptive variability and rates of primary production for Antarctic coastal waters. Over 62% of the variability in PP_{eu} (mg C m^{-2} d^{-1}) can be explained by chl alone (Fig. 2). Only 10% more of the variability in primary productivity (72%) can be explained by using measured C_0 and $E_d(0^+)$ with site-specific parameterizations of the standard depth integrated

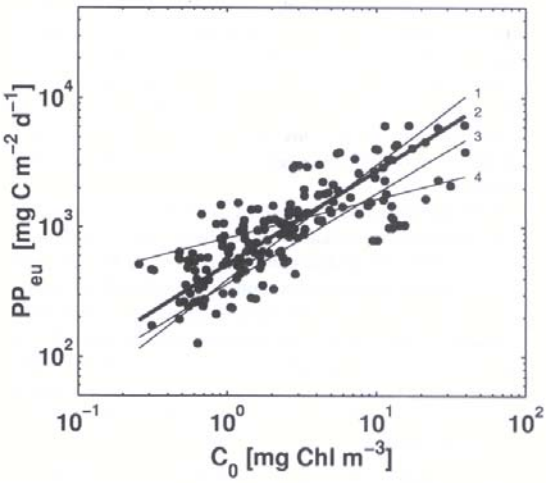

Fig. 11. Best fit relationship between water-column integrated productivity, PP_{eu}, and surface chl, C_0, for: 1) Holm-Hansen & Mitchell (1991) using C_{avg} instead of C_0, 2) These LTER data, such that $PP_{eu} = 512\ C_0^{0.725}$ ($n = 186$, $r^2 = 0.62$), 3) Historic Antarctic data, 4) Bermuda Atlantic Time-Series and Mid-Atlantic Bight data using C_{avg} instead of C_0 (Falkowski *et al.* 1998).

model (Behrenfeld & Falkowski 1997a). Our parameterization of the model (Eq. 7) takes into account three factors that are unique to this region compared to other regions (Behrenfeld & Falkowski 1997b):

1) higher integrated chl concentration predicted from C_0 (Fig. 4),

2) low magnitude of P^B_{opt} (Fig. 5), and

3) more uniform distribution of chl-normalized productivity, which is manifested in the model by a higher F function (Fig. 9).

Not only does this model parameterization perform well on the LTER data from which it was derived, it also explains 73% of the variability in the historic PP_{eu} data collected in these waters (Fig. 10).

A better understanding of P^B_{opt} could potentially improve the model and explain up to 13% more of the variability in PP_{eu}. While low, P^B_{opt} still varies by a factor of seven during the course of a season (Fig. 6). However, no single parameter or group of parameters (e.g. SST, $E_d(0^+)$, chl, daylength, cloud ratio, salinity, mixed layer depth) was found to be a significant predictor of P^B_{opt}. Contrary to expectation, we found no significant relationship between SST and P^B_{opt} (Fig. 7) although, as expected, P^B_{opt} is low compared to global values. In this region, phytoplankton exist in very cold waters and over a relatively restricted range (-2 to 2°C). Furthermore, both diatoms and cryptophytes exhibit a fairly large range in P^B_{opt} (Fig. 8), such that no significant difference was found in the magnitude of P^B_{opt} between these two taxa. Under very large bloom conditions ($C_0 > 10$ mg chl m^{-3}), the phytoplankton in Antarctic coastal waters tend to be diatoms and generally exhibit a lower range of P^B_{opt} centred near the median value of 1.09 mg C mg chl^{-1} h^{-1}.

An interesting result of this analysis is that irradiance seems to play a very limited role in estimating PP_{eu} and only improves the performance of our primary productivity model by 5%. Furthermore, very little correlation was evident between surface irradiance and the photoadaptive variables, P^B_{opt} and F. If these parameters are dependent on enzymatic activity, their variability may depend on temperature and nutrient availability and not adaptations to light (Prezelin *et al.* 1991). Previous experiments on phytoplankton from the cold and often well-mixed waters of the Antarctic have shown them to have slower cellular responses than their temperate counterparts. For example, Antarctic phytoplankton exhibit low respiration rates (Tilzer *et al.* 1986), slow growth rates (Nelson & Smith 1991), and an absence of the ability to repair damage to photosynthetic systems due to UV exposure (Neale *et al.* 1998). Greater understanding of the variability in these photoadaptive parameters could lead to further improvements in the primary production model.

Acknowledgements

This research was supported by NASA Training Grants NGT-40005 (California Space Institute) and NGT5-30063 (Earth System Science Fellowship) to H. Dierssen, National Science Foundation grants OPP90-11927 and OPP-96-32763 to R. Smith and M. Vernet, and NASA grant NAGW 290-3 to R. Smith. We thank Janice Jones, Wendy Kozlowski, Antarctic Support Associates, and the captain and crew of RV *Polar Duke* for their efforts in data collection. We also wish to acknowledge Karen Baker, Sharon Stammerjohn and Charleen Johnson for their help in data processing and manuscript preparation. We also thank the three anonymous referees for their helpful comments.

References

ANTOINE, D. & MOREL, A. 1996. Oceanic primary production: 1. Adaptation of a spectral light-photosynthesis model in view of application to satellite chlorophyll observations. *Global Biogeochemical Cycles*, **10**, 43–55.

ANTOINE, D., ANDRE, J.M. & MOREL, A. 1996. Oceanic primary production: 2. Estimation at global scale from satellite (coastal zone colour scanner) chlorophyll. *Global Biogeochemical Cycles*, **10**, 57–69.

BEHRENFELD, M.J. & FALKOWSKI, P.G. 1997a. Consumers guide to phytoplankton primary productivity models. *Limnology and Oceanography*, **42**, 1479–1491.

BEHRENFELD, M.J. & FALKOWSKI, P.G. 1997b. Photosynthetic rates derived from satellite-based chlorophyll concentration. *Limnology and Oceanography*, **42**, 1–20.

BIDIGARE, R.R., FRANK, T.J., ZASTROW, C. & BROOKS, J.M. 1986. The distribution of algal chlorophylls and their degradation products in the Southern Ocean. *Deep-Sea Research*, **33**, 923–937.

BOOTH, C.R., LUCAS, T.B., MESTECHKINA, R., TUSSON, J.R., NEUSCHULER, D.A. & MORROW, J.H. *eds.* 1995. *NSF Polar Programs UV Spectroradiometer Network 1993–1994 Operations Report* San Diego, CA: Biospherical Instruments, Inc., 167 pp.

BRODY, E., MITCHELL, B.G., HOLM-HANSEN, O. & VERNET, M. 1992. Species-dependent variations of the absorption coefficient in the Gerlache Strait. *Antarctic Journal*, **27**(5), 160–162.

CLAUSTRE, H., MOLINE, M.A. & PREZELIN, B.B. 1997. Sources of variability in the column photosynthetic cross section for Antarctic coastal waters. *Journal of Geophysical Research*, **102**, 25 047–25 060.

EL-SAYED, S.Z. 1978. Primary productivity and estimates of potential yields of the Southern Ocean. *In* MCWHINNIE, M.A., *ed. Polar research: to the present, and the future*, vol. 7. Boulder, CO: Westview Press, 141–160.

FALKOWSKI, P.G., BEHRENFELD, M.J., ESAIAS, W.E., BALCH, W., CAMPBELL, J.W., IVERSON, R.L., KIEFER, D.A., MOREL, A. & YODER, J.A. 1998. Satellite primary productivity data and algorithm development: a science plan for mission to planet earth. *In* HOOKER, S.B. & FIRESTON, E.R., *eds. SeaWiFS Technical Report Series, NASA TM-1998-104566* vol. 42. Greenbelt, MD: NASA/GSFC, Code 970.2, 36.

GAUTIER, C. & FROUIN, R. 1992. Net surface solar irradiance variability in the central equatorial Pacific during 1982–1985. *Journal of Climate*, **5**, 30–55.

GIESKES, W.W.C., KRAAY, G.W., MONTJI, A., SETIAPERMANA, D. & SUMTUMO. 1988. Monsoonal alternation of a mixed and a layered structure in the phytoplankton of the euphotic zone of the Banda Sea (Indonesia): a mathematical analysis of algal pigment fingerprints. *Netherlands Journal of Sea Research*, **22**, 123–137.

GORDON, H.R. & MCGLUNEY, W.R. 1975. Estimation of the depth of sunlight penetration in the sea for remote sensing. *Applied Optics*, **14**, 359–361.

HART, T.J. 1934. On the phytoplankton of the south-west Atlantic and the Bellingshausen Sea, 1929–31. *Discovery Reports*, **8**, 1–268.

HOLM-HANSEN, O. & MITCHELL, B.G. 1991. Spatial and temporal distribution of phytoplankton and primary production in the western Bransfield Strait region. *Deep-Sea Research*, **38**, 961–980.

KOZLOWSKI, W., LAMERDIN, S.K. & VERNET, M. 1995. Palmer LTER: predominance of cryptomonads and diatoms in Antarctic coastal waters. *Antarctic Journal of the United States*, **30**(5), 267–268.

LAWS, E.A. & ARCHIE, J.W. 1981. Appropriate use of regression analysis in marine biology. *Marine Biology*, **65**, 13–16.

LONGHURST, A., SATHYENDRANATH, S., PLATT, T. & CAVERHILL, C. 1995. An estimate of global primary productivity in the ocean from satellite radiometer data. *Journal of Plankton Research*, **17**, 1245–1271.

MARTIN, J.H., GORDEN, R.M. & FITZWATER, S.E. 1990. Iron in Antarctic waters. *Nature*, **345**, 156–158.

MINAS, H.J. & MINAS, M. 1992. Net community production in "high nutrient-low chlorophyll" waters of the tropical and Antarctic Oceans. *Oceanologica Acta*, **15**, 145–162.

MITCHELL, B.G. & HOLM-HANSEN, O. 1991. Observations and modelling of the Antarctic phytoplankton crop in relation to mixing depth. *Deep-Sea Research*, **38**, 961–1007.

MOLINE, M.A. & PREZELIN, B.B. 1996. Long-term monitoring and analyses of physical factors regulating variability in coastal Antarctic phytoplankton biomass, *in situ* productivity, and taxonomic composition over subseasonal, seasonal, and interannual time scales. *Marine Ecology-Progress Series*, **145**, 143–160.

MOLINE, M.A., SCHOFIELD, O. & BOUCHER, N.P. 1998. Photosynthetic parameters and empirical modelling of primary production: a case study on the Antarctic Peninsula shelf. *Antarctic Science*, **10**, 45–54.

MOREL, A. & BERTHON, J.F. 1989. Surface pigments, algal biomass profiles and potential production of the euphotic layer: relationships re-investigated in view of remote sensing applications. *Limnology and Oceanography*, **34**, 1545–1562.

MOREL, A. 1991. Light and marine photosynthesis: a spectral model with geochemical and climatological implications. *Progress in Oceanography*, **26**, 263–306.

NEALE, P.J., DAVIS, R.F. & CULLEN, J.J. 1998. Interactive effects of ozone depletion and vertical mixing on photosynthetsis of Antarctic phytoplankton. *Nature*, **392**, 585–589.

NELSON, D.M. & SMITH, W.O. 1991. Sverdrup revisited: critical depths, maximum chlorophyll levels, and the control of Southern Ocean productivity by the irradiance-mixing regime. *Limnology and Oceanography*, **36**, 1650–1661.

PLATT, T. & SATHYENDRANATH, S. 1988. Oceanic primary production: estimation by remote sensing at local and regional scales. *Science*, **241**, 1613–1620.

PREZELIN, B.B., TILZER, M.M., SCHOFIELD, O. & HAESE, C. 1991. The control of the production processes of phytoplankton by physical structure of the aquatic environment with special reference to its optical properties. *Aquatic Sciences*, **53**, 1015–1621.

PRIDDLE, J., BRANDINI, F., LIPSKI, M. & THORLEY, M.R. 1994. Pattern and variability of phytoplankton biomass in the Antarctic Peninsula region: an assessment of the BIOMASS cruises. *In* EL-SAYED, S.Z., *ed. Southern Ocean ecology: the BIOMASS perspective* Cambridge: Cambridge University Press, 49–126.

SMITH, R.C. 1981. Remote sensing and depth distribution of ocean chlorophyll. *Marine Ecology Progress Series*, **5**, 359–361.

SMITH, R.C., BAKER, K.S. & DUSTAN, P. 1981. *Fluorometer techniques for measurement of oceanic chlorophyll in the support of remote sensing*. San Diego: Visibility Laboratory, Scripps Institution of Oceanography. SIO Ref. 81–17.

SMITH, R.C., EPPLEY, R.W. & BAKER, K.S. 1982. Correlation of primary production as measured aboard ship in southern California coastal waters and as estimated from satellite chlorophyll images. *Marine Biology*, **66**, 281–288.

SMITH, R.C., BAKER, K.S., FRASER, W.R., HOFMANN, E.E., KARL, D.M., KLINCK, J.M., QUETIN, L.B., PRÉZELIN, B.B., ROSS, R.M., TRIVELPIECE, W.Z. & VERNET, M. 1995. The Palmer LTER: a long-term ecological research program at Palmer Station, Antarctica. *Oceanography*, **8**, 77–86.

SMITH, R.C., DIERSSEN, H.M. & VERNET, M. 1996a. Phytoplankton biomass and productivity in the western Antarctic Peninsula Region. *Antarctic Research Series*, **70**, 333–356.

SMITH, R.C., STAMMERJOHN, S.E. & BAKER, K.S. 1996b. Surface air temperature variations in the Western Antarctic Peninsula Region. *Antarctic Research Series*, **70**, 105–122.

SMITH, W.O. & SAKSHAUG, E. 1990. Polar phytoplankton. *In* SMITH, W.O., *ed. Polar Oceanography: Part B chemistry, biology and geology*. San Diego, CA: Academic Press, 477–526.

TALLING, J. 1957. The phytoplankton population as a compound photosynthetic system. *The New Phytologist*, **56**, 133–149.

TILZER, M.M., ELBRACHTER, M., GIESKES, W.W. & BEESE, B. 1986. Light-temperature interactions in the control of photosynthesis in Antarctic phytoplankton. *Polar Biology*, **5**, 105–111.

VERNET, M., KOZLOWSKI, W. & RUEL, T. 1996. Palmer LTER: temporal variability in primary productivity in Arthur Harbor during the 1994/1995 growth season. *Antarctic Journal of the United States*, **30**(5), 266–267.

VOLLENWIEDER, R.A. 1966. Calculation models of photosynthesis-depth curves and some implications regarding day rate estimates in primary production measurements. *In* GOLDMAN, C.R., *eds. Primary productivity in aquatic environments* Berkeley: University of California Press, 425–457.

WATERS, K.J. & SMITH, R.C. 1992. Palmer LTER: a sampling grid for the Palmer LTER program. *Antarctic Journal of the United States*, **27**(5), 236–239.

WRIGHT, J.-C. 1959. Limnology of Canyon Ferry Reservoir: phytoplankton standing crop and primary production. *Limnology and Oceanography*, **4**, 235–245.

ZIMMERMAN, R.C., SOOHOO, J.B., KREMER, J.N. & D'ARGENIO, D.Z. 1987. Evaluation of variance approximation techniques for non-linear photosynthesis-irradiance models. *Marine Biology*, **95**, 209–215.